Journal of Applied Polymer Science

Hydrolysis of polylactide in aqueous media

Edwin J. Rodriguez, Bernard Marcos, Michel A. Huneault
Département de Génie Chimique et de Génie Biotechnologique, Université de Sherbrooke, 2500 Boulevard de l'Université, Sherbrooke Québec J1K 2R1, Canada
Correspondence to: M. A. Huneault (E-mail: michel.huneault@usherbrooke.ca)

ABSTRACT: In this study, two commercial polylactide (PLA) grades with different D-lactate contents were subjected to hydrolysis in neutral, acidic, and alkaline aqueous media at temperatures above the glass transition. We monitored the hydrolysis process by means of tracking the changes in the molecular weight distribution, weight loss, water uptake, and PLA crystallinity as a function of time. In both, neutral and acidic media, hydrolysis showed an initial induction period over which no weight loss was observed, whereas the average molecular weight dropped drastically. After this initial period, the weight loss increased rapidly, whereas the molecular weight decreased slowly. Additionally, in alkaline media, hydrolysis occurred mainly through a surface-erosion process; this resulted in a simultaneous molecular weight decrease and weight loss without a noticeable induction period. An autocatalytic mechanism was assumed in neutral and acidic media to describe the hydrolysis kinetics. The measured molecular weight decrease over time was successfully described by a two-stage exponential model. © 2016 Wiley Periodicals, Inc. J. Appl. Polym. Sci. **2016**, *133*, 44152.

KEYWORDS: degradation; kinetics; polyesters

Received 13 January 2016; accepted 4 July 2016
DOI: 10.1002/app.44152

INTRODUCTION

Polylactide (PLA) is a biobased polyester. It was first used in the medical field for the production of sutures and bioresorbable implants. In the last decade, the large-scale production of PLA from renewable resources has enabled its use in high-volume food-packaging and textile applications.[1,2] PLA is subject to hydrolysis and biodegradation. The biodegradation of PLA is a two-step process that includes an abiotic hydrolysis of the polymer matrix into oligomers and an assimilation of oligomers by microorganisms and their transformation into carbon dioxide and water.[3,4] Abiotic hydrolysis is often considered as the limiting step of PLA degradation. Because PLA is a condensation polymer, chain scission is highly dependent on the presence of water. Water plays an important role by diffusing into the polymer and cleaving ester bonds; this yields carboxyl and hydroxyl end groups. In turn, the carboxyl end groups are capable of catalyzing the further cleavage of other ester bonds. This effect is called *autocatalysis*. The second role of water is in the diffusion of the monomer and water-soluble oligomers produced while hydrolysis proceeds. Oligomers with up to 13 monomers are water soluble.[5] Therefore, when the PLA sample is placed in aqueous media, lactic acid and lactic acid oligomers diffuse through the material and dissolve in water. Diffusion is also assisted by the plasticization effect of water, and this increases the free volume. The extraction of low-molecular-weight species leads to a weight loss in the polymer sample, a phenomenon known as erosion. Depending on the ratio between the diffusion rate and the hydrolysis rate, three erosion mechanisms may arise: surface erosion, bulk erosion, and autocatalytic bulk erosion.[6,7] If water diffusion is slower compared to the degradation rate, hydrolysis and weight loss occur preferentially at the surface, and this leads to surface erosion.[6] If water diffusion is faster than degradation, a uniform weight loss is observed, and this is referred to as *bulk erosion*. However, if the produced monomer and soluble oligomers present in the bulk of a sample cannot diffuse rapidly, their acid end groups will catalyze the reaction and lead to the third mechanism, which is known as *autocatalytic bulk erosion*. In this case, degradation occurs faster in the bulk of the sample than in the outer layer.[8,9]

The kinetics of PLA hydrolysis has been described and studied by many authors.[10–13] The PLA ester bonds are randomly hydrolyzed by water molecules according to the following reaction; this results in carboxylic and hydroxyl end groups:

$$R-C(CH_3)COO-R'+H_2O \rightarrow R-C(CH_3)COOH+HO-R' \quad (1)$$

The simplest hydrolysis kinetics model assumes that the ester-bond breakup rate is proportional to time. Because the number

Additional Supporting Information may be found in the online version of this article

of polymer chains is equal to the number of carboxylic end groups, the hydrolysis reaction can be described by a second-order kinetics model.[14] It is also assumed that at least in the early stages of hydrolysis, the ester and water concentrations are constant and the kinetics can be reduced to pseudo-zero-order kinetics[13,15]:

$$\rho/Mn = \rho_0/M_{n,0} + kt \quad (2)$$

where k is the rate constant, t is the time and M_n and ρ are the number-average molecular weight and polymer density, respectively. The subscript 0 indicates the initial values before hydrolysis. Early studies have shown that the hydrolysis of polyester is autocatalyzed by the carboxylic end groups.[14,15] Because ρ does not change significantly in the early stages of hydrolysis, the kinetics can be described by

$$M_n = M_{n,0}\, e^{-kt} \quad (3)$$

where T is the temperature. The kinetic models represented by eqs. (2) and (3) have been used to describe the hydrolysis of bioresorbable polyesters through the plotting of either $1/M_n$ or $\ln(M_n)$ as a function of time. Although a few authors have compared the two models,[16–18] the majority of published studies have used the autocatalytic model because of its better agreement with experimental data in aqueous media.

PLA hydrolysis is highly temperature dependent.[12,17,19] Hydrolysis is very slow at room temperature under dry conditions. Therefore, most studies have investigated hydrolysis under humid or aqueous conditions and at temperatures near or above the glass-transition temperature (T_g), where macromolecular chains acquire greater mobility. The hydrolysis temperature (T_H) can be classified into three ranges: $T_H < T_g$, $T_g \leq T_H < T_m$, and $T_H > T_m$ (where T_m is the melting temperature).[20] Because of the early interest in PLA for biomedical applications, a large number of publications have covered the hydrolysis of PLA at normal body temperature. One of the difficulties of such experiments is its long duration because hydrolysis at 37 °C can take from many weeks[8,21] to 3 years.[22] Consequently, it has become important to develop accelerated hydrolytic tests at higher temperatures[17,19,21] that can help to predict the behavior of resorbable devices in biomedical applications. Furthermore, rapidly growing biodegradable packaging applications have pointed out the importance of investigating the hydrolysis process at an industrial compost temperature of about 55–60 °C.[23]

The Vogel–Tammann–Fulcher equation describes the effect of the temperature on the rate of hydrolysis above T_g[11]:

$$k = k_0 e^{\frac{-E}{R}\left(\frac{1}{(T-T_s)}\right)} \quad (4)$$

where k_0 and E are the characteristic Vogel–Fulcher–Tammann parameters, R is the ideal gas constant, and T_s is a reference temperature at which the conformational entropy of the polymer chains becomes zero. This reference temperature is often considered to be 50 °C below the T_g.[18,24]

Another influential parameter on PLA hydrolysis is the acidity of the media. Because PLA hydrolysis involves the cleavage of ester groups, the presence of hydronium and hydroxide ions catalyzes the reaction.[20,25] The high concentration of hydroxide ions in alkaline media strongly accelerates the hydrolysis process.[26] However, degradation in alkaline media proceeds via surface erosion rather than by a bulk erosion mechanism as in neutral media.[26]

Most of the literature cited previously has been concerned with the degradation of PLA at low temperatures of around 37 °C because of the interest for PLA in biomedical applications. There have been a few studies in which the degradation at temperatures above PLA's T_g has been investigated. Höglund *et al.*[27] reported degradation kinetics at 37, 60, and 80 °C in terms of the weight loss and M_n evolution. They reported faster degradation in commercial PLA, which comprised a small amount of D-lactate (by opposition to the major L-lactate constituent) in their composition. The D-lactate content is known to drastically reduce the crystalline content of PLA,[28] and therefore, the effect of D-lactate may be indirect, through its effect on the crystalline level of the starting material. The study of Höglund *et al.* was limited to neutral or mildly acidic conditions. In another study from Lyu *et al.*,[12] acid and alkaline media were investigated for a very specific PLA synthesized from a 70/30 DD-lactide/DL-lactide monomer mix. As previous authors noted, Lyu *et al.* noted that the rapid molecular weight decreased under aggressive conditions, and a certain induction time before sample weight loss occurred. Interestingly, they proposed a time–temperature superposition scheme to predict the temperature effects. Among the large body of work from the group of Tsuji *et al.*,[19] the effect of the crystallinity on the degradation of PLA at elevated temperatures was also investigated. The study was carried out on thin films synthesized solely of LL-lactide, and they showed a similar molecular weight evolution but slower weight loss with highly crystalline samples.

The objective of this study was to further improve our understanding of the degradation kinetics at elevated temperature. In particular, this study focused on commercial PLA (with D-content limiting crystallization) rather than on pure PLA. The degradation of thick, melt-processed samples in contrast to solution cast films is also addressed. The examination of thick samples enabled differentiation between the surface and bulk erosion trough microscopic examination of the samples. Highly acid and alkaline conditions were also investigated. These conditions are of interest if PLA is to be subjected to aggressive environments in an accelerated test for screening PLA formulations or from a fundamental perspective to illustrate the shift from a bulk erosion mechanism to a surface-erosion mechanism as the medium becomes more aggressive.

Although there have been studies that have evaluated the effect of different parameters on PLA hydrolysis, few of them have combined multiple effects simultaneously. Accordingly, the general context of this study was to investigate PLA hydrolysis and PLA crystallinity development at a higher temperature relevant to industrial composting (>55 °C and high humidity) or in more aggressive media relevant to a chemical recycling process requiring accelerated hydrolysis. The hydrolysis in aqueous media of semicrystalline and amorphous PLA grades was studied between 60 and 80 °C and at pH values between 1

Table I. Molecular Characteristics of the PLAs before Hydrolysis

PLA grade	D-Lactate (%)	M_n (g/mol)	M_w (g/mol)	M_w/M_n	T_g (°C)	T_m (°C)
4032D (cPLA)	2	106,000	168,000	1.58	61	166
8302D (aPLA)	10	88,000	146,500	1.66	59	—

and 12. Therefore, hydrolysis was examined at much higher temperatures and under more extreme pH conditions than what can be found in life-science-oriented studies.

EXPERIMENTAL

Materials and Sample Preparation

Two commercial grades (4032D and 8302D) of PLA (NatureWorks LLC) were used. These were selected because they differed widely in D-isomer content. PLA 4032D had around 2% D-lactate and could crystallize upon cooling, whereas 8302D comprises a larger amount of D-lactate, about 10%, and was, therefore, fully amorphous under normal conditions. Hereafter, the crystalline and amorphous grades are called cPLA and aPLA, respectively. The main molecular characteristics of these grades are summarized in Table I. Before molding, the materials were dried in a vacuum oven at 40 °C for 24 h. Subsequently, the dried PLA pellets were compression-molded at 200 °C in the form of 25 mm diameter disk samples with an approximately 2 mm thickness and an approximate weight of 1.1 g. The samples were rapidly cooled down to room temperature under pressure inside the compression-molding press through an integrated cold-water recirculating system. The overall cooling time was 6 min.

Hydrolysis

The hydrolysis experiments were carried out in 50 mL centrifugal tubes containing 30 mL of hydrolysis media for a predetermined duration and at various temperatures. A first set of experiments was carried out in distilled water with pH 5.4. Three temperature values were chosen, that is, 60 °C (because of its relation to the composting temperature), 70 °C, and 80 °C, to determine the kinetic constants. To ensure the greatest hydrolysis progress, the maximum duration of the hydrolysis was set accordingly to 50, 30, and 15 days, respectively. To investigate the effect of pH, additional experiments were carried out in acidic and alkaline conditions at pH values of 1, 9, and 12. The temperature was set at 70 °C, and the hydrolysis was monitored for 10 days. The pH level of the aqueous and moderately alkaline media, that is, pH 5.4 and 9, was measured each 24 h before its renewal with fresh distilled water or alkaline solution, depending on the case. Whenever the hydrolysis was performed in alkaline conditions, that is, pH 12, the complete renewal of the hydrolysis media was done as soon as the pH level was varied by 0.5 units. The acidic hydrolysis media was not renewed because its pH level did not change significantly. All experiments were performed in triplicate, the mean was reported, and the standard deviation was plotted.

Weight Loss Measurement

Samples removed from the hydrolysis media were wiped dry and weighed to determine the wet weight. The samples were afterward dried for 5 days at 40 °C in a vacuum oven. The weight of the dried samples (W_{dry}) was then measured, and the total weight loss of the samples was calculated as follow:

$$\text{Weight loss} = \left[\left(\frac{W_0 - W_{dry}}{W_0}\right)\right] \times 100 \quad (5)$$

where W_0 is the initial sample weight. Similarly, the water uptake was calculated with the weight of the wiped discs after hydrolysis (W_{wet}) and W_{dry}:

$$\text{Water uptake} = \left[\left(\frac{W_{wet} - W_{dry}}{W_{dry}}\right)\right] \times 100 \quad (6)$$

Molecular Weight Characterization

The molecular weight characterization was performed for the original and hydrolyzed PLA discs via gel permeation chromatography with an Agilent 1100 high-performance liquid chromatography series instrument equipped with Agilent ResiPore columns and a refractive-index detector. Tetrahydrofuran at 40 °C was used as the mobile phase at a flow rate of 0.6 mL/min, and the columns were calibrated with polystyrene standards. Three samples were taken and dried at the end of each hydrolysis step. Before gel permeation chromatography analyses, these samples were dissolved in tetrahydrofuran between 30 and 40 °C and subsequently filtered by means of a 0.45-μm filter.

Thermal Characterization

The thermal properties of PLA samples, such as T_g, T_m, and the melting enthalpy, were characterized through nonisothermal analyses with a TA Instruments Q2000 differential scanning calorimeter. Samples cut from the dried hydrolyzed and original PLA molded discs were heated from 10 to 200 °C at a rate of 20 °C/min under a nitrogen gas flow. To assess the direct effect of hydrolysis on the thermal properties of PLA, only the first heating scan was considered.

Rheological Characterization

The relationship between the molecular weight and the viscoelastic properties of the hydrolyzed PLA samples was investigated through rheological characterization. The original PLA discs and those subjected to hydrolysis for 8, 16, and 24 h at 60 and 70 °C were characterized. The measurements were carried out in dynamic small-amplitude oscillatory shear mode with a stress-controlled Anton Paar MCR 502 rheometer at 180 °C with 25-mm parallel-plate geometry. To hinder the further oxidation and thermal degradation of PLA, experiments were done under a nitrogen atmosphere.

Scanning Electron Microscopy (SEM) Micrographs

SEM micrographs of the hydrolyzed sample surfaces were carried out to better understand the erosion mechanism. The micrographs were obtained with a Hitachi S-3000N scanning electron microscope in high-vacuum mode at a voltage of 5 kV. The samples were sputtered with gold beforehand at 25 mA.

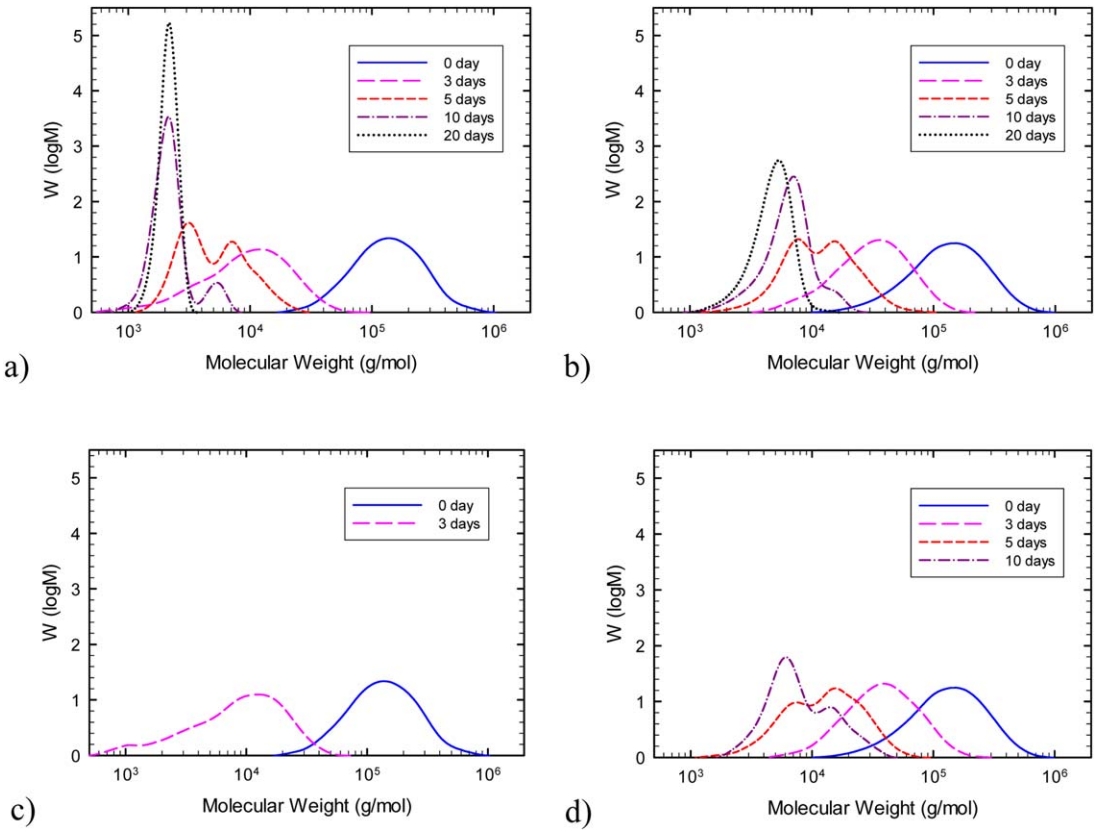

Figure 1. Molecular weight distribution (Mass fraction W for constant molar mass increments log M) of PLA hydrolyzed at 70 °C for (a) aPLA at pH 5.4, (b) cPLA at pH 5.4, (c) aPLA at pH 12, and (d) cPLA at pH 12. [Color figure can be viewed in the online issue, which is available at wiley onlinelibrary.com.]

RESULTS AND DISCUSSION

Molecular Weight Distribution Evolution

Hydrolysis decreases the molecular weight and alters the molecular weight distribution of PLA. The evolution over time of the molecular weight distribution of PLA in aqueous media at pH 5.4 and 12 at 70 °C is presented in Figure 1 (other media are shown in the Supporting Information). Regardless of the PLA grade, the molecular weight distribution shifted to lower molecular weights and transformed into a bimodal distribution at the intermediate hydrolysis time. For example, for pH 5.4, at early stages of hydrolysis, that is, up to 3 days, a monomodal distribution was observed. This was gradually transformed into a bimodal distribution between the 5th and 10th day of hydrolysis. In the late stages of hydrolysis, that is, after the 20th day, once again, a narrow monomodal molecular weight distribution with a polydispersity index close to 1 appeared. The same monomodal/bimodal transitions were found when PLA was subjected to pHs of 1 and 9, but the duration of the experiments was not long enough to reach the narrow monomodal regimes (Figure S1 in the Supporting Information). Similar trends were also observed for hydrolysis taking place at 60 and 80 °C. The behavior for aPLA at pH 12 was somehow different. The sample volume varied appreciably during hydrolysis. The weight loss was directly related to visual observation of the thickness and diameter reduction of the samples; this suggested a surface-erosion mechanism. As the temperature increased, the degradation rate increased, too, and the transitions between monomodal and bimodal distributions shifted to earlier stages of hydrolysis. The bimodal distribution has been repeatedly associated with heterogeneous degradation when autocatalytic bulk erosion is present.[27] However, autocatalytic bulk erosion was reported even in the absence of bimodal distribution.[21]

Hydrolysis in Neutral Media: Temperature Effect

Temperature accelerates the hydrolysis of PLA. To evaluate this effect, hydrolysis in aqueous media was carried out at 60, 70, and 80 °C. The evolution of the molecular weight, weight loss, and water uptake are presented in Figure 2 for aPLA and cPLA, respectively. Unless stated otherwise, the samples were fully amorphous at the start of the hydrolysis process. For the data at 60 °C, however, we compared the evolution observed for cPLA that was fully crystallized (i.e., annealed) before hydrolysis to the behavior of the amorphous sample (i.e., quenched). The melting enthalpy before hydrolysis for the annealed cPLA was about 45 J/g.

At all temperatures, no weight loss occurred initially during the period that we refer to as the *induction period*. After this period, the weight loss followed an S-shaped curve, and the molecular weight continued to decrease but at a lower rate. During the induction period, the molecular weight dropped dramatically from 100 kg/mol to the 10–20 kg/mol range. This induction period also coincided with the monomodal molecular weight distribution mentioned previously. The induction time was strongly decreased as a function of the temperature, and it was

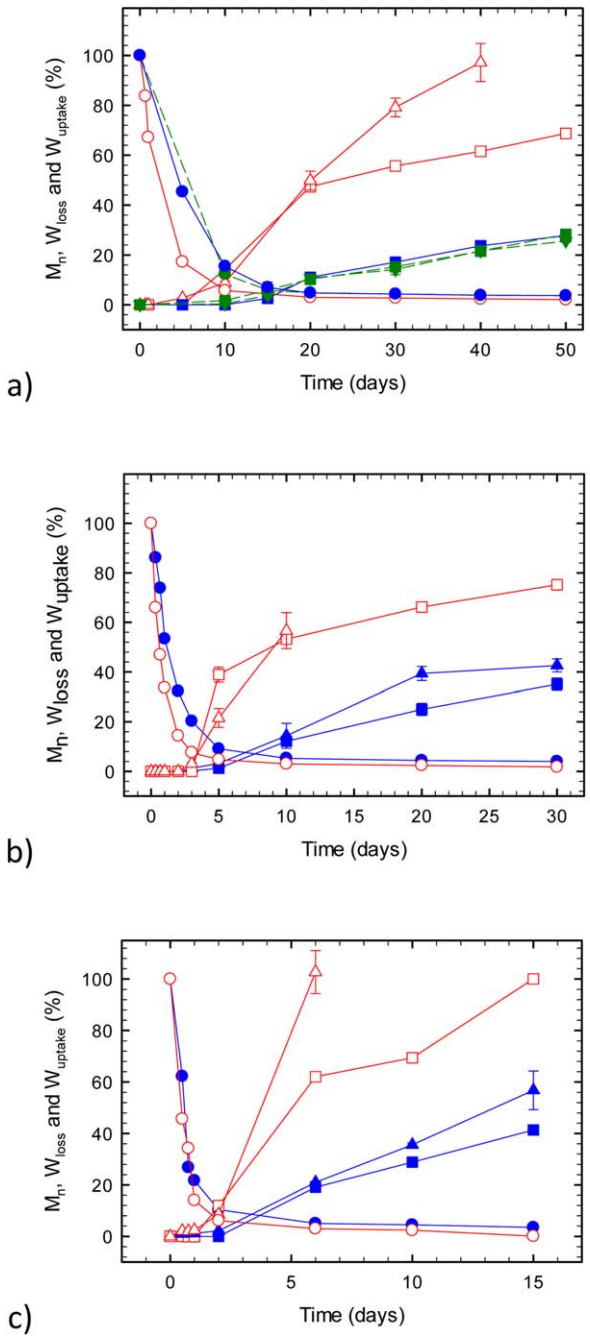

Figure 2. (•) M_n, (■) weight loss (W_{loss}), and (▲) water uptake (W_{uptake}) during PLA hydrolysis at pH 5.4 at different temperatures: (a) 60, (b) 70, and (c) 80 °C. Unfilled symbols indicate aPLA, and filled symbols indicate cPLA. At 60 °C (in dashed green), the quenched cPLA was compared with the annealed cPLA. [Color figure can be viewed in the online issue, which is available at wileyonlinelibrary.com.]

also dependent on the PLA grade. For example, this period corresponded to 5, 3, and 1 days for aPLA and 10, 3–5, and 2 days for cPLA at 60, 70, and 80 °C, respectively. In the second stage, the weight loss began abruptly. During this period, the molecular weight decrease rate progressively slowed down; this was most likely due to the decrease in the ester link concentration and the loss of the autocatalysis effect. In terms of the time required to reach a weight loss of 50% of aPLA, it was around 23, 8, and 5 days at 60, 70, and 80 °C. The experiment duration was not sufficient for obtaining the half-life of cPLA. Nevertheless, the weight loss of cPLA showed a very similar behavior at all temperatures. In other words, after the induction stage, the weight loss began rapidly and followed a characteristic S-shaped curve. Surprisingly for cPLA, the prior annealing of the samples did not lead to an increased hydrolytic stability. In contrast to the usual belief that the kinetics of crystallization and those of hydrolytic degradation were closely coupled, these observations showed that for crystallizable PLA, the initial crystalline state of the sample did not play an important role.

Another variable used to monitor the hydrolysis process shown in Figure 2 was the water uptake. The water uptake provided another measure of the polymer morphology. The weight loss by bulk erosion increased the porosity of the polymer matrix. Consequently, more water could enter these pores, and in turn, this promoted autocatalysis and weight loss. Interestingly, the water-uptake behavior was always closely linked to the weight loss. For example, the water uptake was nearly zero during the induction stage, and this closely followed the weight loss curve during the second hydrolysis regime. The higher weight loss of aPLA was also reflected in a greater water uptake. This information was important because it confirmed that erosion did occur within the core of the sample through nonhomogeneous hydrolysis and the creation of autocatalytic pockets, which led to the creation of an interconnected porosity.

Hydrolysis in Acid and Alkaline Media: pH Effect

Figure 3 summarizes the molecular weight decrease (M_n), weight loss, and water uptake during the hydrolysis of aPLA and cPLA at 70 °C in more aggressive acid and alkaline media at pH 1 and 12 (see Figure S2 in the Supporting Information for the data at pH 9). At pH 1 and 9, the overall observations were similar to those made for hydrolysis in distilled water, namely, a rapid initial molecular weight decrease and an induction period in terms of weight loss. Also, as for distilled water experiments, the amorphous aPLA showed a faster weight loss than the semicrystalline cPLA. The induction time was not altered significantly by strongly acidic or weakly alkaline media. Finally, the good match between the absorbed water and weight loss was maintained. Quantitatively, the weight loss of aPLA observed after 10 days at pH 9 was higher, about 70%, than the weight loss observed in distilled water or at pH 1, about 50%. This confirmed that the alkaline media favored the hydrolysis, as pointed out earlier. The results were dramatically different at pH 12. First, weight loss started immediately without any induction stage and was carried out in parallel to the molecular weight reduction. Second, the weight loss occurred much more rapidly. For example, it took only 3 days to reach 80% weight loss of the aPLA. For cPLA, similar weight loss occurred in around 5 days. Furthermore, the weight loss and water absorption were not fully correlated at pH 12 as the weight loss proceeded much more rapidly than the water uptake. This observation, combined with the readily visible sample size reduction over the course of the hydrolysis experiment, suggested that in the highly alkaline media, although bulk erosion was always present, surface erosion played a dominant role. The

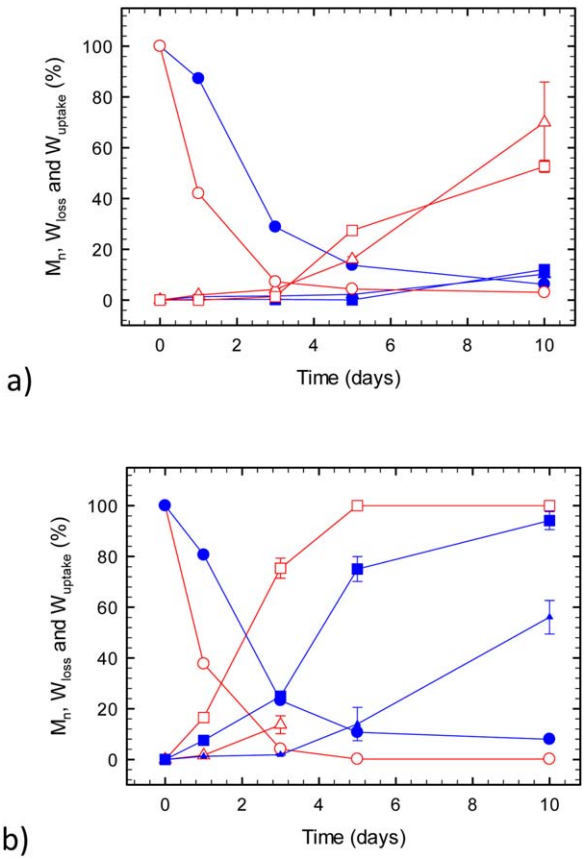

Figure 3. (●) M_n, (■) weight loss (W_{loss}), and (▲) water uptake (W_{uptake}) during PLA hydrolysis at 70 °C in different media at pH (a) 1 and (b) 12. Unfilled symbols indicate aPLA, and filled symbols indicate cPLA. [Color figure can be viewed in the online issue, which is available at wileyonlinelibrary.com.]

cleavage of ester bonds in low-viscosity oils is known to be very rapid in the presence of caustic soda, and it is used, for example, in saponification reactions. In these experiments, the surface reaction was initiated as soon as the sample was placed in the media; this led to immediate weight loss. It should be noted that some internal cavitation, related to bulk erosion, seemed to occur as well; this was evidenced by the water-uptake increase after an induction of 1 and 3 days for aPLA and cPLA, respectively. Therefore, after sufficient time for diffusion within the sample, both the surface and bulk erosion contributed to hydrolysis. This was confirmed by SEM micrographs performed on PLA sample surfaces. Figure 4 shows the micrographs of the cPLA surface before and after hydrolysis under alkaline and neutral media at 70 °C. Figure 4(a) shows the surface before hydrolysis. This surface was relatively smooth. After 1 day of hydrolysis in the alkaline media, cavities already appeared on the surface, as shown in Figure 4(b). These cavities could have been associated with the 7% weight loss already attained at this point. M_n was still very high at 85% of its original value. At the 5th day, the surface was highly cavitated [Figure 4(c)] with a wide distribution of cavity sizes. At that point, the weight loss reached approximately 75%, and M_n decreased to approximately 11% of its original value. By contrast, the cPLA surfaces after a 10-day exposure to neutral media, shown in Figure 4(d), exhibited a significantly different behavior. Despite the fact that M_n decreased to approximately 5% of its original value and 12% of the sample weight was lost, no cavities were found on the sample surface. Additionally, Figure 5 presents SEM micrographs taken on the fracture surfaces in the bulk of the hydrolyzed sample in alkaline and neutral media at 70 °C. Figure 5(a,b) shows the bulk surface after 3 days of hydrolysis in alkaline media and after 20 days in neutral media, respectively. The two samples were selected for comparison because they both lost approximately 25% of their original weight. The fracture surfaces in the bulk were quite different. The fracture surface for the alkaline media sample was smooth because most of the weight loss occurred from the surface rather than from the bulk of the sample. The micrograph from the sample hydrolyzed in the neutral media showed a very irregular surface topology, and more interestingly, it clearly showed hexagonal patterns that were left by spherulitic structures. The most probable explanation was that amorphous regions located between the spherulites were preferentially hydrolyzed. Therefore, the fracture occurred between the remaining spherulites. This clearly indicated than in the neutral media, the hydrolysis proceeded more or less uniformly in the bulk of the material. This pointed to the major difference in the erosion mechanism and the fact that essentially in alkaline conditions, the surface and bulk erosion proceeded simultaneously, whereas in neutral and acid media, it was mainly the bulk erosion mechanism that was responsible for the weight loss.

Crystallization

Hydrolysis in aqueous media resulted in some changes in the PLA crystallinity. Figure 6 presents the differential scanning calorimetry heating thermograms obtained from aPLA and cPLA after being subjected to an increasing number of days in distilled water at 70 °C. The 0-day result was for the molded sample before any contact with the aqueous media. As expected, the aPLA exhibited a clear glass transition around 57 °C and no trace of any cold crystallization or melting at higher temperatures. The cPLA did not achieve any crystallinity upon molding because it was rapidly cooled from the melt state. It was, nonetheless, crystallizable, and its heating thermograms exhibited a glass transition (~61 °C); this was followed by a broad exothermic peak due to cold crystallization, which was followed by a small endothermic melting peak centered at 165 °C. The melting enthalpy (area under the peak) was similar to the crystallization enthalpy; this indicated that the cPLA was initially fully amorphous. Surprisingly, the aPLA after 3 days in distilled water at 70 °C exhibited a clear dual-melting peak (117 and 128 °C). This dual-melting endothermic increased in size after 5 days of hydrolysis and turned into a single peak after a longer hydrolysis. This single peak clearly shifted to lower temperatures between the 10th and 30th day of hydrolysis. Lower T_m values were typically associated with less perfect crystal structures and to thinner crystalline lamellar thicknesses. Possibly, some racemization occurred in the material over time. The same behavior was found for samples hydrolyzed at 60 and at 80 °C. The crystallization of aPLA was unexpected because this material did not develop a crystalline structure before hydrolysis, even after

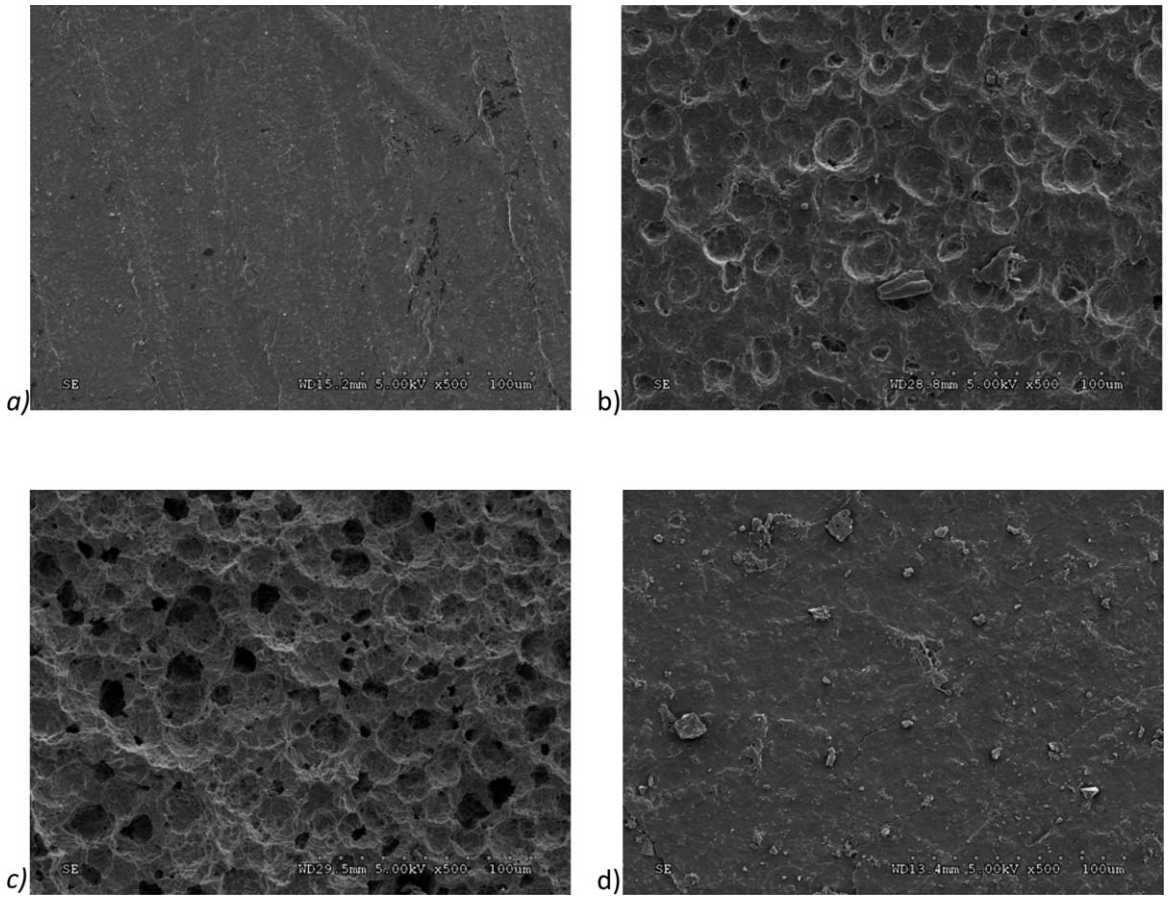

Figure 4. SEM micrographs of the cPLA sample surfaces before and after hydrolysis at 70 °C: (a) before hydrolysis, (b) after 1 day in an alkaline medium, (c) after 5 days in an alkaline medium, and (d) after 10 days in a neutral medium.

annealing for several days. In this situation, however, the extended period under which the material was annealed over its T_g; the high water content, which could have plasticized the material; and the molecular weight loss, all contributed to reduce the dynamic barrier to crystallization. Because the aPLA contained a higher fraction of D-lactate units, which acted as crystal defects, the crystalline lamellae were smaller and less stable. In the case of cPLA, the immersion in aqueous media led to the disappearance of the small crystallization peak and the creation of a sharper melting peak at 147 °C. Thus, the period in the aqueous media enabled the full crystallization of the sample. The melting peak also shifted to a lower temperature when the hydrolysis experiment proceeded but at a lower rate than for the aPLA. The melting enthalpy remained nearly constant. We envisioned that more perfect crystals were unaffected by hydrolysis but that as amorphous chain segments got cleaved, the crystals progressively reorganized into smaller crystals and lower T_m crystals.

Figure 7 illustrates the melting enthalpy and T_m as a function of the molecular weight during hydrolysis at all temperatures. The melting enthalpy was increased by hydrolysis for both aPLA and cPLA. Before the hydrolysis, all samples were in the amorphous state. For aPLA, the first sign of crystallization appeared when M_n was reduced to approximately 40,000 g/mol. This was confirmed by the opacity of the samples. At this stage, no weight loss had occurred. A low melting enthalpy value of 3.8 J/g was achieved, with two melting peaks appearing at 122 and 133 °C. When the weight-average molecular weight (M_w) was decreased to 2.8 kg/mol, one single T_m was found (121 °C), and the melting enthalpy was significantly increased to approximately 52 J/g. T_m was further reduced to 88 °C when M_w decreased to approximately 1.6 kg/mol. The behavior of cPLA was slightly different because only one T_m value was found for all M_w values. Before hydrolysis, cPLA showed a T_m value of 166 °C, but no crystallinity was initially present, as evidenced by the fact that the melting enthalpy was equal to the crystallization exotherm. When the molecular weight was decreased to about 4.0 kg/mol, T_m reached 145 °C. The enthalpy development and T_m changes were independent of the pH of the media (Figure S3, Supporting Information). The cPLA crystallized quickly during hydrolysis; a melting enthalpy of 25 J/g was reached ($M_w \approx$ 92 kg/mol) in just a few hours after the samples were immersed in the hydrolysis media. When the molecular weight was decreased further to about 4.0 kg/mol, the melting enthalpy increased to about 70 J/g. This was a very high value for cPLA because upon slow cooling or annealing under dry conditions (i.e., without hydrolysis), the maximum melting enthalpy for this material was around 45 J/g.

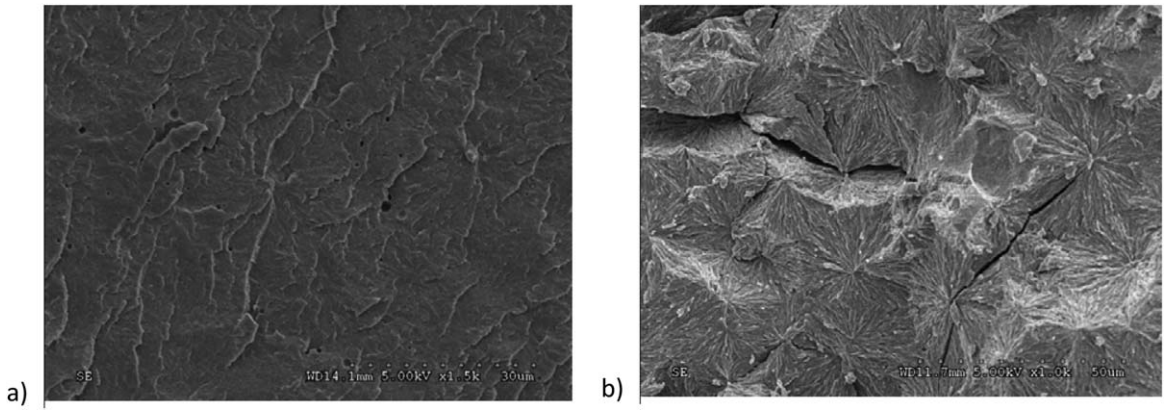

Figure 5. SEM micrographs of the cPLA fracture surfaces before and after hydrolysis at 70 °C: (a) after 3 days in an alkaline medium and (b) after 20 days in a neutral medium.

Rheology–Molecular Weight Relationship

The rheological behavior of the polymer melt was strongly affected by the molecular weight. At molecular weights below the critical entanglement molecular weight, the polymer viscosity was proportional to M_w. For molecular weights above the critical entanglement molecular weight, the polymer viscosity is known to obey a power law relation, with the viscosity increasing proportionally to M_w^n, where n is an exponent reported to be approximately 3.4 for linear polymers.[29] Elastic relaxation of the polymer will also be affected in the same way with the relaxation time increasing with M_w. The plateau viscosity is presented as a function of M_w for aPLA and cPLA in Figure 8. A power law relation was observed, as expected. Regardless of the hydrolysis conditions, the data fell on a single curve. The power law exponent (n) was 3.95. This value was slightly higher than the 3.4–3.7 power found by Dorgan *et al.*,[30,31] but it was in agreement with the 4.0 found by Cooper-White and Mackay.[32]

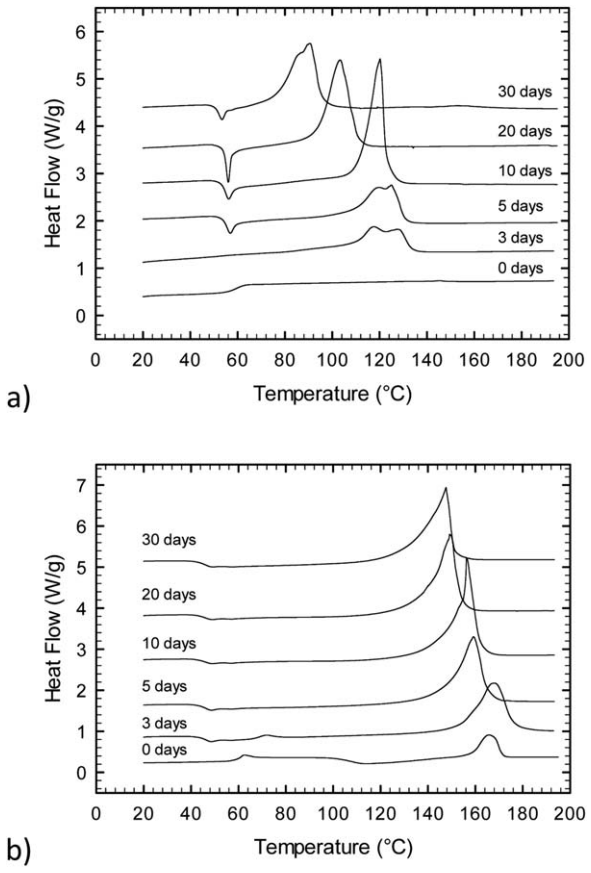

Figure 6. Differential scanning calorimetry thermograms of the samples hydrolyzed in neutral media at 70 °C: (a) aPLA and (b) cPLA.

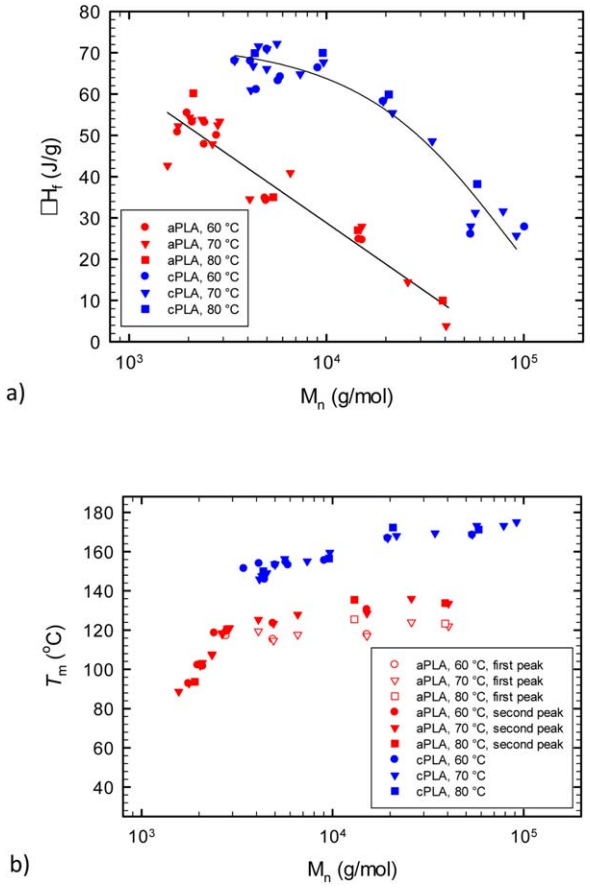

Figure 7. (a) Enthalpy of fusion (ΔH_f) and (b) T_m as a function of M_n of the neutral media at 60, 70, and 80 °C. [Color figure can be viewed in the online issue, which is available at wileyonlinelibrary.com.]

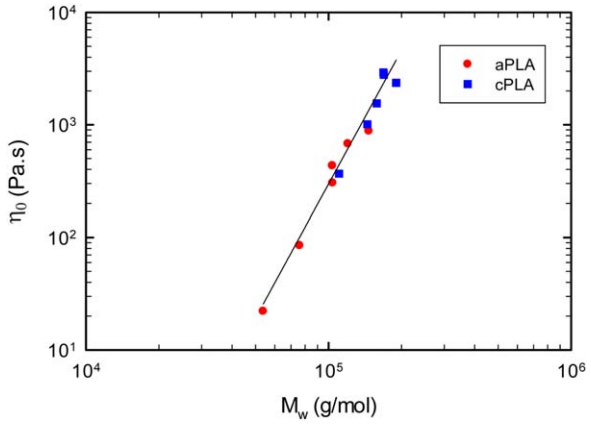

Figure 8. Viscosity (η_0) as a function of the molecular weight for the hydrolyzed PLA samples. [Color figure can be viewed in the online issue, which is available at wileyonlinelibrary.com.]

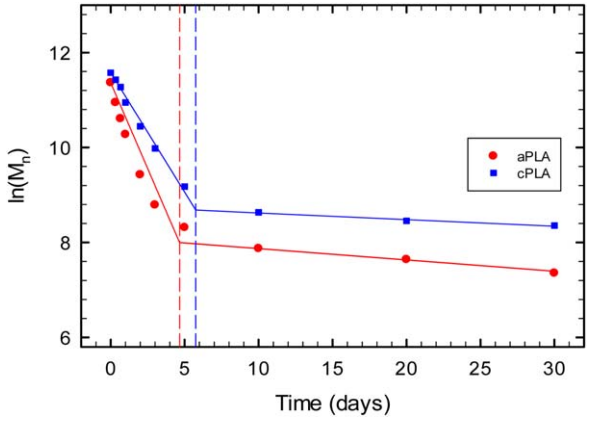

Figure 9. M_n data versus the PLA hydrolysis time at 70 °C in neutral media: aPLA and cPLA. [Color figure can be viewed in the online issue, which is available at wileyonlinelibrary.com.]

Kinetic Analysis

The molecular weight data (M_n) versus the hydrolysis time in aqueous media for each temperature were analyzed. The three kinetic models described earlier were able to describe the hydrolysis behavior, but for simplicity, pseudo-first-order kinetics were assumed [cf. eq. (3) in the Introduction]. Figure 9 presents the molecular weight as a function of the hydrolysis time for PLA hydrolyzed in distilled water at 70 °C. Because an exponential relation was expected, the data were plotted in the log-normal scale. According to this figure, a shift in the kinetic rate was observed during the PLA hydrolysis. Two linear portions were found; these corresponded to the following relationships:

$$M_n = \begin{cases} M_{n0_1} e^{-k_1 t} & \text{if } t < t_p \\ M_{n0_2} e^{-k_2 t} & \text{if } t > t_p \end{cases} \quad (7)$$

where M_{n0_1} is the molecular weight before hydrolysis, M_{n0_2} is the number-average molecular weight intercept of the second hydrolysis stage, k_1 and k_2 are the kinetic constants for each stage, and t_p is the shift time between the two stages.

The first stage was characterized by a reaction rate that was one to two orders of magnitude greater than that in the second phase. The same behavior was observed at 60 and 80 °C (Figure S4 in the Supporting Information). This behavior could be explained by observation of the weight loss trend. At the beginning, the induction stage took place, and no weight loss occurred. The polymer chains reacting in the bulk of the sample contributed to the autocatalytic effect, and the reaction was accelerated. In contrast, when the weight loss began, the molecular weight was already reduced by almost 85%. This led to a reduction in the ester link concentration and a decrease in the autocatalytic effect, which were caused by water dilution and the extraction of low-molecular-weight lactic acid oligomers. It should be noted that once the oligomers were removed by dissolution in the media, the low-molecular-weight portion of the distribution was automatically subtracted. In addition to the actual molecular weight reduction by hydrolysis, this effect artificially reduced the kinetics because we could no longer account for the lower M_w species. Nevertheless, eq. (3) has been used as a useful tool for kinetics modeling by others.[12,16,23]

The kinetic parameters in aqueous media are summarized in Table II. As expected, the kinetic constants showed a progressive increase with temperature. The kinetic constant increased by a factor of 2.5 when the temperature was increased by 10 °C. With respect to the PLA grade, the aPLA kinetic constants proved not to exceed 1.7 times the corresponding constants for cPLA. In general, the kinetics rates were in the same order of magnitude as those observed in other reports at similar temperatures.[11,22]

The temperature dependence of hydrolysis kinetics in aqueous media has been modeled with the Vogel–Tammann–Fulcher equation [cf. eq. (4)]. The two kinetic constants at the three temperatures were used to calculate the parameters of the Vogel–Tammann–Fulcher equation, and these are presented in Table III. The kinetic parameters k_{0i} and $(E/R)_i$ were calculated

Table II. Kinetic Parameters of the Autocatalytic Model for PLA Hydrolysis in Aqueous Media

PLA grade	Temperature (°C)	$k_1 \times 10^2$ (days^{-1})	$k_2 \times 10^2$ (days^{-1})	M_{nO2} (g/mol)	t_p (days)
aPLA	60	30.0	1.28	3390	11.2
	70	72.2	2.38	3323	4.7
	80	152.2	5.84	3858	1.9
cPLA	60	18.1	0.90	5961	16.7
	70	50.4	1.39	6363	5.7
	80	125.4	4.23	6303	2.2

Table III. Vogel–Tammann–Fulcher Equation Parameters for PLA Hydrolysis in Aqueous Media

	$(E/R)_1$ (K)	k_{01} (days^{-1})	R^2	$(E/R)_2$ (K)	k_{02} (days^{-1})	R^2
aPLA	388.4	191.6	0.99	358.7	4.72	0.96
cPLA	463.1	397.0	0.99	362.3	3.31	0.89

Table IV. Kinetic Constant of the Pseudo-First-Order Model for PLA Hydrolysis at Various pHs and 70 °C

PLA grade	aPLA				cPLA			
pH	1	5.4	9	12	1	5.4	9	12
$k_1 \times 10^2$ (days^{-1})	68.2	72.2	65.6	98.9	44.7	50.4	44.2	49.9

via the fitting of the data in a linear plot; the subscript i represents each kinetic stage (1 or 2), and T_s was assumed to be 273 K (see Figure S5 in the Supporting Information). Despite the fact that only three temperature values were used for this study, the first kinetic stage for both aPLA and cPLA fit the VFT equation ($R^2 \sim 1$). For the second kinetic phase, aPLA fit better than cPLA. With respect to the order of magnitude, the results were consistent with those of prior studies. For example, for aPLA, we found that the E/R factors were 388.4 and 358.7 K for the first and second kinetic stages, respectively, whereas Lyu *et al.*[11] found an intermediate value of 379 K for the hydrolysis of amorphous PLA over a temperature range from 37 to 90 °C.

The media effect on the hydrolysis kinetics was studied. Hydrolysis at 70 °C in three media was used to determine the kinetic parameters. The data of M_n versus time for 5 days of hydrolysis were fitted with the pseudo-first-order kinetics [cf. eq. (3)]. The k_1 values, for both aPLA and cPLA, at four pH values are summarized in Table IV. For pH values of 1, 9, 5.4, and 12, the calculated kinetic constants confirmed that the pH did not significantly affect the hydrolysis rate, as already mentioned previously (Figure S6 in the Supporting Information). Only the aPLA at pH 12 showed a remarkable acceleration. The hydrolysis rate of aPLA was around 1.4 times faster than those at the other pH values. However, this rate was not sufficient to justify the total weight loss in 5 days; this supported the assumption that in the strongly alkaline media, degradation proceeded mainly by a surface-erosion mechanism.

CONCLUSIONS

The hydrolysis of PLA in aqueous media was investigated by the monitoring of changes in the sample weight, water uptake, molecular weight distribution, melting enthalpy, and T_m. Except in a very alkaline medium (pH 12), the hydrolysis process of PLA proceeded in two stages through a bulk erosion mechanism. The first stage was characterized by a fast molecular weight decrease, the appearance of a dual-peak molecular weight distribution, and also a stable PLA sample weight. The second stage was characterized by a slower molecular weight change, which was accompanied by a gradual sample weight loss, because of the dissolution of low-molecular-weight PLA oligomers into the aqueous media. A porous structure was illustrated by the fact that in this stage, the sample was able to absorb a significant amount of water into its interconnected pore network. By contrast, in the highly alkaline media, it was shown that PLA hydrolysis occurred mainly through a surface-erosion mechanism. In this case, the alkaline medium reacted directly with the sample surface; this led to little or no induction period in terms of weight loss and to an observable sample size reduction.

The degradation of amorphous and semicrystalline PLA grades (i.e., grades differing in optical purity) was investigated. The degradation of the amorphous grade was found to be slightly faster than that of the crystallizable PLA grade, but the two materials exhibited very similar responses to changes in the media acidity and media temperature. The semicrystalline PLA samples were intentionally molded into amorphous disks through rapid cooling. The semicrystalline PLA rapidly developed its crystalline structure during the hydrolysis experiments, as expected, because the hydrolysis was carried out above the PLA T_g. However, the crystallinity level that could be attained during the hydrolysis was much higher than that typically attained in crystallization from the melt state. We assessed this by heating the PLA samples in a differential scanning calorimeter. Melting endotherms (upon heating in a differential scanning calorimeter) in excess of 70 J/g were attained. Surprisingly, even the so-called amorphous grade PLA developed a crystalline structure when it was placed in aqueous media. This probably contributed to the levelling out of the differences in terms of the degradation rate between the amorphous and semicrystalline grades. Finally, the molecular weight change was easily correlated with the melt viscosity measurements. The power law relation $\eta_0 = M_w^{3.95}$ was found to be in agreement with the expected behavior for linear polymers above their critical entanglement molecular weight.

REFERENCES

1. Avérous, L. *Monomers Polym. Compos. Renew. Resour.* **2008**, 433.
2. Garlotta, D. J. *Polym. Environ.* **2001**, *9*, 63.
3. Premraj, R.; Doble, M. *Indian J. Biotechnol.* **2005**, *4*, 186.
4. Gautam, R.; Bassi, A. S.; Yanful, E. K. *Appl. Biochem. Biotechnol.* **2007**, *141*, 85.
5. Höglund, A.; Hakkarainen, M.; Edlund, U.; Albertsson, A.-C. *Langmuir* **2010**, *26*, 378.

6. Göpferich, A. *Polym. Scaffolding Hard Tissue Eng.* **1996**, *17*, 103.
7. Burkersroda, F. V.; Schedl, L.; Göpferich, A. *Biomaterials* **2002**, *23*, 4221.
8. Li, S. M.; Garreau, H.; Vert, M. J. *Mater. Sci. Mater. Med.* **1990**, *1*, 123.
9. Grizzi, I.; Garreau, H.; Li, S.; Vert, M. *Biomaterials* **1995**, *16*, 305.
10. Pitt, C. G. *Spec. Publ. R. Soc. Chem.* **1992**, *109*, 7.
11. Zhang, X.; Wyss, U. P.; Pichora, D.; Goosen, M. F. A. *J. Bioact. Compat. Polym.* **1994**, *9*, 80.
12. Lyu, S. P.; Schley, J.; Loy, B.; Lind, D.; Hobot, C.; Sparer, R.; Untereker, D. *Biomacromolecules* **2007**, *8*, 2301.
13. Farrar, D. in Degradation Rate of Bioresorbable Materials; F. J. Buchanan, Ed.; Woodhead Publishing: Cambridge, UK, **2008**; Chap. 9, pp 183–206.
14. Pitt, C. G.; Gratzl, M. M.; Kimmel, G. L. *Biomaterials* **1981**, *2*, 215.
15. Siparsky, G. L.; Voorhees, K. J.; Miao, F. J. *Environ. Polym. Degrad.* **1998**, *6*, 31.
16. Weir, N. A.; Buchanan, F. J.; Orr, J. F.; Dickson, G. R. *Proc. Inst. Mech. Eng. Part H* **2004**, *218*, 307.
17. Weir, N. A.; Buchanan, F. J.; Orr, J. F.; Farrar, D. F.; Dickson, G. R. *Proc. Inst. Mech. Eng. Part H* **2004**, *218*, 321.
18. Lyu, S.; Sparer, R.; Untereker, D. J. *Polym. Sci. Part B: Polym. Phys.* **2005**, *43*, 383.
19. Tsuji, H.; Nakahara, K.; Ikarashi, K. *Macromol. Mater. Eng.* **2001**, *286*, 398.
20. Tsuji, H. In Poly(lactic acid): synthesis, structures, properties, and applications; Auras, R. A., Lim, L.-T., Selke, S. E. M., Tsuji, H., Eds.; Wiley: Hoboken, NJ, **2010**; Chap. 21, pp 347–376.
21. Li, S.; McCarthy, S. *Biomaterials* **1999**, *20*, 35.
22. Tsuji, H.; Ikada, Y. *Polym. Degrad. Stab.* **2000**, *67*, 179.
23. Gorrasi, G.; Pantani, R. *Polym. Degrad. Stab.* **2013**, *98*, 1006.
24. Gibbs, J. H.; DiMarzio, E. A. *J. Chem. Phys.* **1958**, *28*, 373.
25. Tsuji, H.; Nakahara, K. *J. Appl. Polym. Sci.* **2002**, *86*, 186.
26. Tsuji, H.; Ikada, Y. *J. Polym. Sci. Part A: Polym. Chem.* **1998**, *36*, 59.
27. Höglund, A.; Odelius, K.; Albertsson, A.-C. *ACS Appl. Mater. Interfaces* **2012**, *4*, 2788.
28. Saeidlou, S.; Huneault, M. A.; Li, H.; Park, C. B. *Prog. Polym. Sci.* **2012**, *37*, 1657.
29. Dorgan, J. R. In Poly(lactic acid): Synthesis, Structures, Properties, Processing, and Applications; Auras, R. A., Lim, L.-T., Selke, S. E. M., Tsuji, H., Eds.; Wiley: Hoboken, NJ, **2010**; p 125.
30. Dorgan, J. R.; Lehermeier, H.; Mang, M. *J. Polym. Environ.* **2000**, *8*, 1.
31. Dorgan, J. R.; Janzen, J.; Clayton, M. P.; Hait, S. B.; Knauss, D. M. *J. Rheol.* **2005**, *49*, 607.
32. Cooper-White, J. J.; Mackay, M. E. *J. Polym. Sci. Part B: Polym. Phys.* **1999**, *37*, 1803.